Agricultural and Forest Meteorology 340 (2023) 109601

Contents lists available at ScienceDirect

Agricultural and Forest Meteorology

journal homepage: www.elsevier.com/locate/agrformet

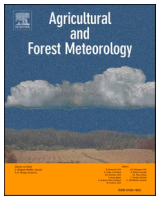

Detecting the long-term spatiotemporal crop phenology changes in a highly fragmented agricultural landscape

Biniam Sisheber [a,b,*], Michael Marshall [a], Daniel Mengistu [b], Andrew Nelson [a]

[a] Department of Natural Resources, Faculty of Geo-information Science and Earth Observation (ITC), University of Twente, Hallenweg 8, 7522 NH Enschede, the Netherlands

[b] Geospatial Data and Technology Center (GDTC) and Department of Geography and Environmental Studies, Bahir Dar University, Bahir Dar, Ethiopia

ARTICLE INFO

Keywords:
agriculture, food security, phenometrics interannual variations, ESTARFM, remote sensing

ABSTRACT

Trends in crop phenometrics reveal the influence of climate variability and change on crop growth and development. However, the trends are less clear in fragmented tropical smallholder landscapes, because there is high spatial and temporal variability in crop phenology. Frequent historical and high spatial resolution (≤30 m) Earth observations are needed to track changes in crop phenology in fragmented landscapes but are often unavailable. The spatial–temporal gap can be closed by integrating infrequent high spatial resolution Earth observations with low spatial/high temporal resolution observations through data fusion. We fused 30 m resolution Landsat and 250 m resolution MODIS imagery to investigate trends in crop phenology from 2000 to 2020 in a fragmented agricultural landscape of Ethiopia. We used the Enhanced Spatial and Temporal Adaptive Reflectance Fusion Model (ESTARFM) that had recently been modified for application in fragmented agricultural landscapes. We used the non-parametric Mann–Kendall test for crop phenology trend analysis. Crop phenology based on Landsat–MODIS fusion was compared to MODIS-based crop phenology without fusion. We found data fusion yielded a smaller magnitude of changes in the start of season (SOS: -0.2-day-y^{-1}) and end of season (EOS: -0.50-day-y^{-1}) compared to MODIS SOS (-0.5-day-y^{-1}) and EOS (1.38-day-y^{-1}) due to MODIS-related mixing with the surrounding natural vegetation in the fragmented agricultural landscape. EOS showed a faster rate of change compared to SOS over the 21-years. The Landsat and MODIS fusion captured spatial variation in the timing and magnitude of change specific to crops and their growing environment, which has implications for adaptation strategies. Our results highlight the importance of long-term data fusion to improve the spatial dimension of crop phenology time series analysis. Integrating time series land cover maps into the data fusion processing chain could further improve long-term data fusion for crop phenology trend analysis.

1. Introduction

Agricultural production in smallholder farming systems faces enormous challenges because of climate variability, extreme weather events, soil degradation, rapid population growth, and inequitable land tenure (Brown et al., 2010; Place, 2009). These problems remain the major drivers of poor agricultural production and the sources of food insecurity in Africa (Nakalembe et al., 2021). Understanding the changes in crop phenology (i.e., the timing and duration of crop development stages) provides essential information on the effect of climate variability on crop growth and production to address food insecurity. However, in various smallholder farming communities, monitoring the small (<1ha) and fragmented crop fields is difficult, which hinders our understanding of crop phenology dynamics (Bolton et al., 2020).

Earth observations monitor crop phenology changes over large areas and over time (Yang et al., 2020). However, historical records, high spatial resolution (≤30 m), and frequent observations (≤8 days) are needed to monitor crop phenology changes in heterogeneous agricultural landscapes (Li et al., 2017; Whitcraft et al., 2015b). The most important crop phenological parameters (hereafter phenometrics) include: start of season (SOS) or the emergence date; the end of the season (EOS) or harvest date; and peak of growth (POS) (Mishra et al., 2021). Global and regional analyses of vegetation change using coarse spatial resolution Earth observation widely reported advance SOS and delay EOS in most croplands in the northern hemisphere (Brown et al., 2012; Chen et al., 2021; Liu et al., 2017; Yang et al., 2021). However,

* Corresponding Author
E-mail address: b.s.tilahun@utwente.nl (B. Sisheber).

https://doi.org/10.1016/j.agrformet.2023.109601
Received 20 September 2022; Received in revised form 3 July 2023; Accepted 10 July 2023
Available online 12 July 2023

studies based on coarse spatial and temporal resolution data correlate poorly with field-level crop statistics (Chen et al., 2021). Similarly, in Africa, vegetation community-level studies using coarse spatial resolution data showed inconsistent spatial and temporal patterns in the timing of crop phenology and the magnitude of its change (Adole et al., 2018a; Alemu and Henebry, 2017; Meroni et al., 2014). This has been attributed to high landscape heterogeneity caused by complex topography, small and irregularly shaped fields, double and mixed cropping practices, and inter-annual rainfall variability.

High spatial and temporal resolution information is important to reveal the long-term and environment-specific crop phenology changes in fragmented landscapes in Africa but are often unavailable (Nakalembe et al., 2021). The daily and 8/16-day composites Moderate Resolution Imaging Spectoradiometer (MODIS) (250–500 m) data, for example, is unable to discern field-level variations and is only meaningful in areas of homogeneous crop-type cover (Tian et al., 2013; Whitcraft et al., 2015a). On the other hand, Landsat provides the longest, continuous historical satellite record at 30 m spatial resolution, which is appropriate to identify and monitor fragmented agricultural landscapes; however, the 16-day temporal resolution is not appropriate for tracking crop growth (Roy et al., 2016). Moreover, persistent cloud cover becomes a challenge to acquire adequate cloud-free images to monitor crop growth (at least every 8-days) in most tropical rainfed agriculture when using Landsat data for crop phenology trend analysis (Whitcraft et al., 2015b). The fusion of Landsat and MODIS data is an opportunity to analyse long-term crop phenology trends due to the availability of historical observations and the complementary nature of the datasets (Gao et al., 2015).

Spatiotemporal data fusion integrates high (low) spatial resolution and low (high) temporal resolution data to obtain frequent high spatial resolution historical records for crop phenology trend analysis (Tian et al., 2013). However, few studies have employed data fusion for continuous and long-term trend analysis. Those that have done so were conducted at temperate latitudes, where croplands are relatively homogeneous, fields are large, and cloud-free input imagery is readily available. Gao et al. (2017) fused Landsat and MODIS from 2001 to 2014 at three-year intervals to analyze crop phenology variation in the US Corn Belt region. Schmidt et al. (2015) generated a 12-year time-series of Landsat–MODIS fused data in Queensland, Australia, to monitor forest disturbance. Using 11 years of Landsat and MODIS fusion, Tian et al. (2013) captured field-level vegetation change in the Loess Plateau, China. These studies, which were conducted for short periods and on natural vegetation, revealed relatively stable temporal dynamics. It is therefore important to evaluate the feasibility of data fusion for longer-term (2000 to 2020) crop phenology trend analysis in fragmented tropical (cloudy) agricultural landscapes that are dominated by smallholder farmers.

The inherent limitation of data fusion algorithms to capture inter-annual and land cover changes could result in spurious trends, when frequent cloud-free Landsat inputs are unavailable (Knauer et al., 2016). Choosing the appropriate data fusion algorithm for fragmented agricultural landscapes is crucial to capture both spatial and temporal growth changes through data fusion (Nietupski et al., 2021). The enhanced (E) STARFM (Zhu et al., 2010) performed favorably in heterogeneous environments but was unable to capture temporal change in crops. In a recent study (Sisheber et al., 2022), ESTARFM was modified to capture the spatial and temporal variation in crops by using crop calendar information to identify and distribute input images and a land cover map to select similar pixels from homogenous land cover classes. The model was evaluated using ground sowing and harvest date information, and the modified model prediction error was 7 days RMSE for SOS and 10 days for EOS compared to 17 days for the SOS and EOS based on MODIS. ESTARFM also captured field-level crop phenology that could provide opportunity to investigate the long-term crop phenology change in fragmented agricultural landscapes.

In this study, we investigated the long-term crop phenology trend in a fragmented tropical agricultural landscape in Ethiopia between 2000 and 2020. We used Landsat and MODIS fusion to reveal the spatial and temporal patterns of SOS, POS and EOS changes specific to crops, which is important for informing climate adaptation and mitigation planning. We compared trends in crop phenometrics as detected by Landsat and MODIS data fusion with those detected using MODIS alone to assess the contribution of data fusion to discern crop phenometric change from the surrounding natural vegetation in a fragmented agricultural landscape. The main contribution of our approach is the derivation of a long-term (>20-years) crop phenology trend at high spatial resolution (30m) using Landsat–MODIS data fusion.

2. Study Area

The study covers crop growing districts surrounding the Lake Tana sub-basin in Ethiopia (Fig. 1), a major agroecosystem for staple grains (teff, maize, millet, and rice). The elevation ranges from 1700 to 3500 meters, mean above sea level. The mean annual average temperature and cumulative precipitation range from 13°C to 22°C and 970 mm to 1900 mm, respectively. The main rainy season (locally called *kiremt,* or summer) occurs between June and September. It supports the main (*meher)* cropping season. The northward movement of the inter-tropical convergent zone (ITCZ) drives *kiremt* rainfall. A short and highly variable rainfall period (*belg* or spring) also occurs between March and May, while October to January (*bega* or winter) is the dry season that also influences *meher* crop production (Gummadi et al., 2018). Crops are sown between June and early August and harvested between November and mid-December. Crop production is mainly rainfed and stratified by climatology and topography. The highlands surrounding the basin are dissected plateau and receive the largest amount of rainfall. Here, fields are small (<1ha), and the main crops are millet and teff. The central districts (Bahir Dar Zuria, Dera, and Mecha) consist of plains and undulating topography that support maize and teff cultivation. Rice is cultivated in the lowland floodplain east of Lake Tana (Fogera and Kemkem).

3. Data and Methods

Fig. 2 illustrates the main inputs, processes, and outputs of the technical workflow of the study. First, we fused the red and near-infrared bands of Landsat and MODIS using ESTARFM between 2000 and 2020. Then EVI2 computed from the fused and MODIS time-series was used to detect crop phenology in TIMESAT (Eklundh and Jönsson, 2017). A crop mask classified in 2019 from Landsat data was used to identify the crop pixels. Finally, we analyzed the trends in crop phenology over 21 years.

3.1. Data acquisition and processing

3.1.1. Landsat

We acquired level-2 terrain corrected surface reflectance red and near-infrared spectral bands for 2000 to 2020 from the United States Geological Survey (USGS) Earth Explorer (https://earthexplorer.usgs.gov) for path/row: 170/52 of Landsat-5 Thematic Mapper (TM), Landsat-7 Enhanced Thematic Mapper (ETM+), and Landsat-8 Operational Land imager (OLI). The images were atmospherically corrected with the Landsat-8 Surface Reflectance Code (LaSRC), improved aerosol determination for Landsat-8, and the Landsat Ecosystem Disturbance Adaptive Processing System (LEDAPS) for Landsat-5 and Landsat-7 (Roy et al., 2016). As Landsat-5 imagery was unavailable from 2003 to 2009, we used Landsat-7 imagery, and applied the local linear histogram-matching method developed by the USGS (Hossain et al., 2015) to fill gaps (SLC-off). We selected relatively low Landsat cloud cover scenes ≤30%, for input and 30-70% for validation after assessing of proportion of cloud-free pixels within the study boundary and used the Landsat pixel quality to mask cloud pixels because of the absence of

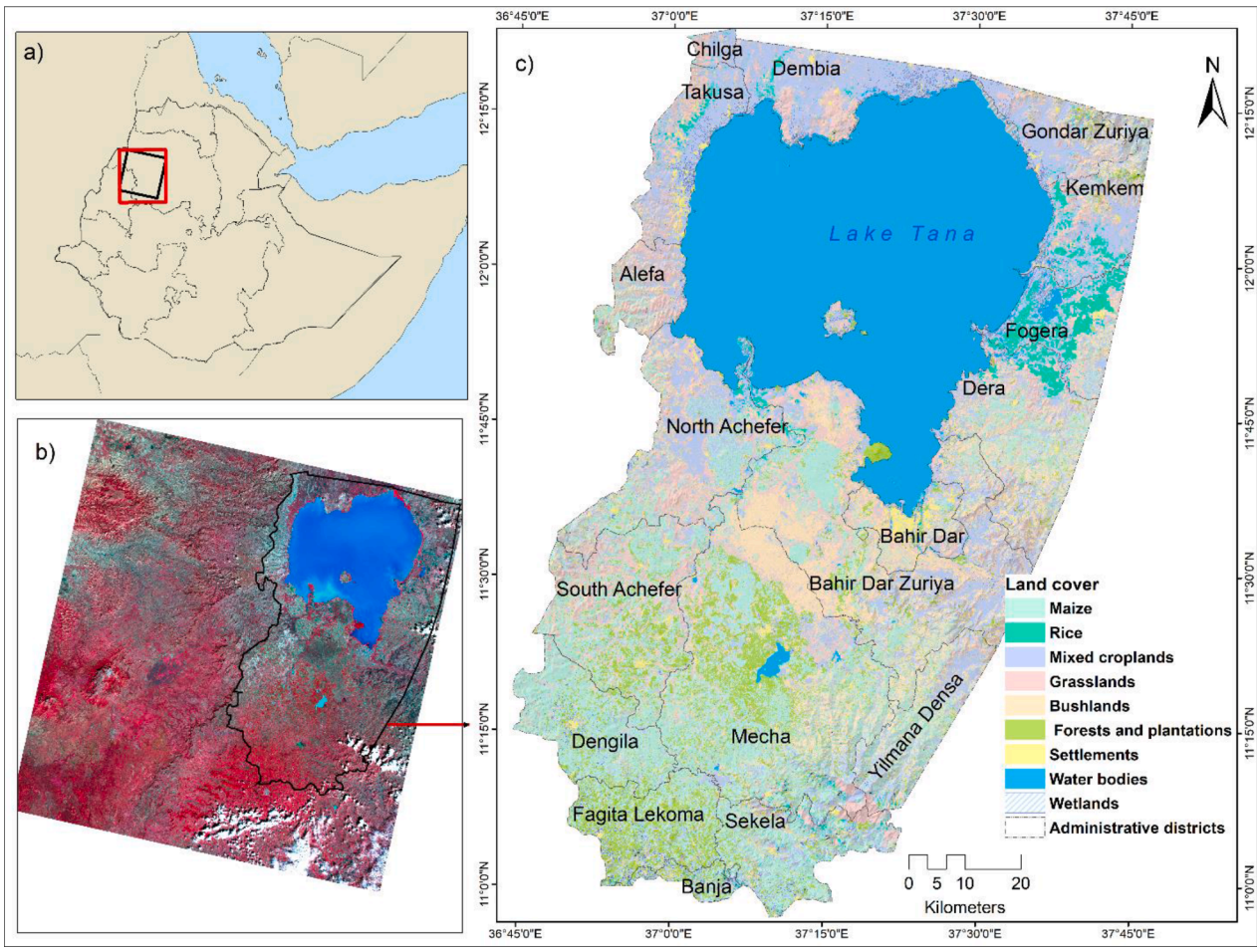

Fig. 1. Location of the study area within Ethiopia (a). NIR-red-green Landsat-8 (path/row: 170/52 of November 30, 2019) false-colour composite shows the spatial coverage of the study area (b). Land cover map of the study area (c) for the 2019 growing season adapted from Sisheber et al. (2022).

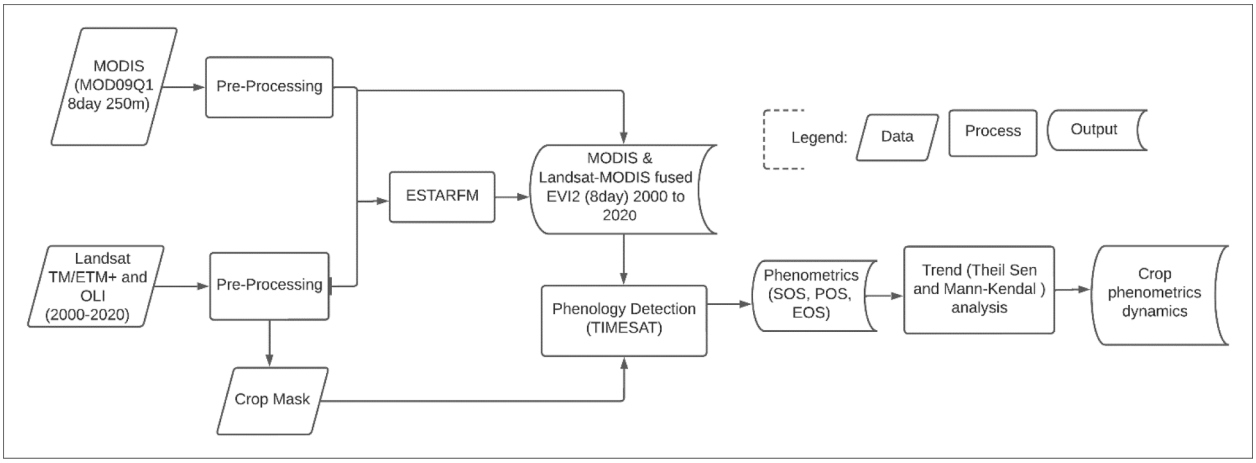

Fig. 2. Technical workflow of the methodology. Landsat and MODIS fused through ESTARFM and crop mask classified in 2019 (Sisheber et al., 2022) used to identify crop pixels for trend analysis.

cloud-free images. Fig. 3 provides the distribution of Landsat inputs during the growing season over the 21-years data fusion period.

3.1.2. *MODIS*

We used the MODIS surface reflectance data (MOD09Q1:V006) acquired from NASA's LPDAAC website (https://lpdaac.usgs.gov) for image tile: 21/7 horizontal/vertical over the study period. The product consisted of atmospherically and aerosol corrected red and near-infrared spectral bands at 250 m spatial resolution composited over 8-day intervals, which is important for improving data fusion for crop phenology monitoring in fragmented landscapes (Wang et al., 2017). The MODIS Sinusoidal projection was re-projected to WGS84 UTM zone 37 and resampled to 30 m using nearest neighbor to match the Landsat projection and spatial resolution. We used the MODIS state-quality flag to

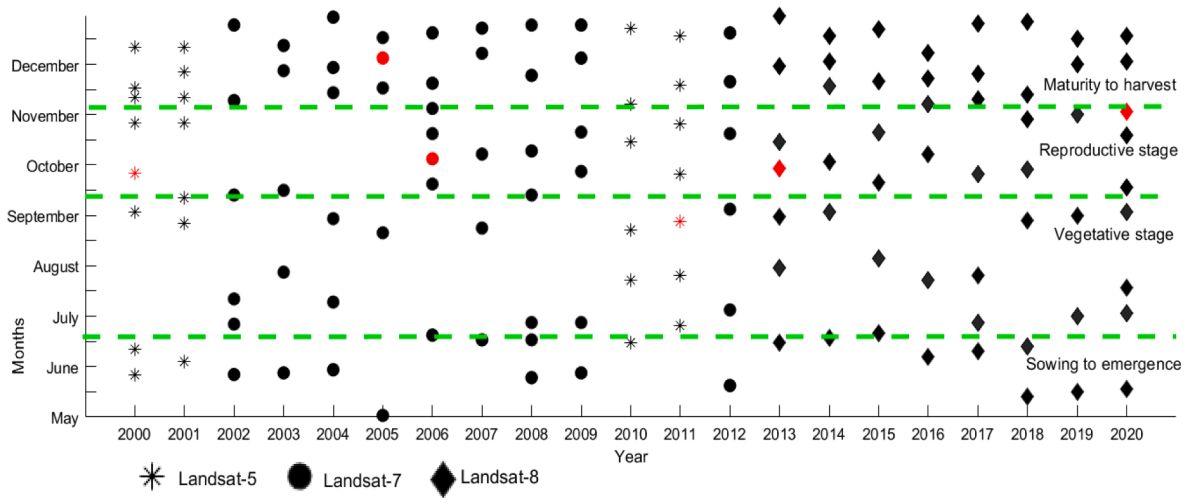

Fig. 3. Distribution of Landsat input images identified from the onset of the main crop growing season (May) to harvest (December). The black colour represents data fusion inputs and the red colour represents validation inputs.

omit cloud and cloud shadow pixels from the trend analysis.

3.1.3. Crop mask

We used a land cover map (Fig. 1) classified in 2019 with Landsat-8 (Sisheber et al., 2022) to filter croplands and categorize maize (2120 km^2), rice (258 km^2), mixed croplands (2168 km^2), natural vegetation classes (3736 km^2), water bodies (3103 km^2), and built-up areas (199 km^2). The cropland accounts for 39% of the land cover. An accuracy assessment using ground truth data showed that the classified map had an overall accuracy of 82.9%, a kappa coefficient of 0.80, a user's accuracy of 79%, and a producer's accuracy of 78%. The location and extent of croplands in Ethiopia is largely defined by climate and topography (Evangelista et al., 2013).Change occurs gradually over the years (Mohammed et al., 2020). To validate this, we randomly sampled 750 cropland points and visually analyzed them using historical Google Earth images between 2000 and 2020. Of these, 90% of the sample points were evaluated as stable cropland throughout the study period. To minimize the 10% error, we eliminated pixels with a high coefficient of variation (CV> 20%) of the phenometrics that could indicate land cover change, similar to the approach used by Qader et al. (2015).

3.2. Analytical techniques

3.2.1. Landsat–MODIS data fusion

We used ESTARFM (Zhu et al., 2010), modified for fragmented agricultural landscapes (Sisheber et al., 2022), to fuse Landsat (TM/ETM+ and OLI) and MODIS imagery from 2000 to 2020. ESTARFM uses two pairs of Landsat and MODIS images at the base date (t_0:t_1 & t_2) and MODIS images at the prediction dates (t_p) to predict high-resolution Landsat–MODIS fused (hereafter fused) data. We distributed the available Landsat inputs at the vegetative, reproductive, and maturity stages based on the dominant crop (maize and rice) calendar of the study area (Fig. 3) to minimize the effect of reflectance change between t_0 and t_p (see,Sisheber et al., 2022). When frequent cloud-free Landsat inputs were available, we selected the Landsat and MODIS inputs at the same acquisition dates. When the available cloud free Landsat inputs are at different phenological stages of crops, we used the MODIS composite best correlated with MODIS input at t_p and with Landsat at the base dates (MODIS t_0-t_p correlation) to compensate for phenology change. We used 128 Landsat inputs for fusion and six for validation (Fig. 3). Then, similar pixels were searched for based on the intersection of Landsat reflectance at t_1 and t_2 in a moving window (w) size of 50 × 50 Landsat pixels and homogeneous land cover class (c). We used the land cover map (Fig. 1) as input to select similar pixels from the same land cover class. Due to the small field size and variation of management practice, adequate similar pixels (>20 pixels) were obtained when c=6 for vegetative growth stage prediction and c=4 during the other periods. Finally, we calculated the spatial weighting function (w_i) and conversion coefficient (v_i) by applying the original ESTARFM (Zhu et al., 2010) to predict fused images for 21 years at 8-day intervals per year using Eq. 1.

$$L\left(x_w/2, y_w/2, t_p, b\right) = L(x_w/2, y_w/2, t_0, b) + \sum_{i=1}^{N} w_i * v_i * \left(M\left(x_i, y_i, t_p, b\right) - - M(x_i, y_i, t_0, b)\right) \quad (1)$$

where L and M denote Landsat and MODIS pixels at coordinates x_i and y_i and band (b), $x_w/2$, $y_w/2$ are the coordinates of the central pixel. N and w_i are the numbers of similar pixels in a moving window used to create the weight and coefficient of the i^{th} date of prediction. We implemented the fusion in IDL® (Interactive Data Language).

We computed the two-band enhanced vegetation index (EVI2) (Jiang et al., 2008) from the fused and MODIS time-series (eq. 2) for crop phenology trend analysis because it is less sensitive to soil background and does not saturate for dense vegetation (Yang et al., 2020). For spatial consistency, the MODIS EVI2 was resampled at 30 m spatial resolution. A linear correlation of EVI2, determined from independent Landsat images reserved for validation and fused images, was used to evaluate the inter-annual data fusion performance (see Supplementary data, Fig.S1).

$$EVI2 = 2.5\left(\frac{\rho NIR - \rho Red}{1 + \rho NIR + 2.4\rho Red}\right) \quad (2)$$

Ideally, Landsat missions are consistent and comparable, allowing for continuous time-series analysis. However, incremental developments in sensors, data transmission, acquisition, and processing could influence the interpretation of Landsat time-series. Thus, the

combined use of Landsat-5, -7, and -8 data requires further harmonization. To this end, we obtained 15 images from overlapping Landsat scenes (row/Path: 169/52) and calculated EVI2 on cloud-free sample pixels. Then all the time-series EVI2 were transformed to Landsat-7 values using linear transformation as proposed by Roy et al. (2016). The equations for data harmonization are:

$$LS7 = 0.023637 + 0.933630 * EVI2_{LS5} \ldots\ldots (R2 = 0.83, P \leq 0.01, n = 195174) \quad (3)$$

$$LS7 = 0.023464 + 0.895451 * EVI2_{LS8} \ldots\ldots (R2 = 0.84, P \leq 0.01, n = 228229 \quad (4)$$

where LS7, LS5 and LS8 represent the EVI2 derived from Landsat-7, -5, and -8. For *n* cloud-free sample pixels, high R^2 at p ≤0.01 was obtained to convert Landsat-5 and -8 values to Landsat-7 values.

3.2.2. Crop phenometrics

The TIMESAT software package was used to calculate phenometrics. We first smoothed the EVI2 time-series using the Savtizky–Golay (S–G) filter Eklundh and Jönsson, 2017) to minimize the impact of atmospheric effects and data fusion inconsistencies. We used the MODIS quality flag to define the influence (weight) of pixels as 1.0 (full contribution) for cloud-free, 0.0 (no contribution) for cloudy pixels, and 0.5 (reduced contribution) for medium cloud and cloud shadow probability pixels. For each year, the second upper envelope iteration, adaptive strength ((3), and window size (4) were used for fitting. From the fitted fused EVI2 time-series, the SOS and EOS were extracted using the seasonal amplitude (dynamic threshold) method, as this method takes account of crop characteristics (Yang et al., 2020). We used thresholds of 10% and 30% of the seasonal amplitude to determine the SOS and EOS respectively. The time at the apex of the fitted curve was the POS (EVI2max date). Crop phenometrics were also extracted from MODIS to assess how the fusion improved our understanding of cropland phenology dynamics. The crop phenometrics detection were fine-tuned and tested using sowing and harvest date information collected from 17 maize and 16 rice fields (see supplement, Table S1) randomly identified in the study area, and found that data fusion performed well than MODIS (Sisheber et al., 2022). We used bias, root mean square error (RMSE) and coefficient of determination (R^2) to assess the deviation and error between the fused and MODIS phenometrics. The 21-years mean phenometrics were aggregated at pixel level to understand the spatial distribution of crop phenology.

3.3. Crop phenology trend analysis

The crop phenology trend was determined from fused and MODIS derived phenometrics for comparison. We used the timing of SOS, EOS, and POS in the trend analysis for pixels (n=1,648,020) within the crop mask area over the study period (2000 to 2020). A 4-year temporal filter, considering the average crop rotation period, based on a Gaussian weighted mean, was applied to exclude outliers and minimize the likelihood of a spurious trend (Schmidt et al., 2012). We applied the non-parametric Theil–Sen (TS) median slope estimator to investigate the magnitude of crop phenology change and the Mann–Kendall (MK) test (Eastman et al., 2013) to test the significance of the trend. Unlike the slope of linear regression, the TS estimator and MK test are recommended for remote sensing time-series analysis because of their insensitivity to outliers and occasional missing data and do not require a normally distributed time-series (Marshall et al., 2016). Thus, for every pixel with a valid retrieval of SOS, EOS, and POS, the slope of pairwise combinations $n(n-1)/2$ was computed, and the median value estimates the rate of change. The slope above zero indicates a positive trend; the slope below zero indicates a negative trend. The MK test statistics consists of calculating the Kendall Score (S:Eq. 5) and its variance (var) (Jong et al., 2012). S denotes the sign of data values (xj), and n is the number of years (21). The test statistics Z-score was calculated (Eq. 6), and the result was classified as a significant increase/decrease based on the level of confidence to show spatial variation of phenological change (Table 1). An MK z-score ≥±1.96 indicates a significant increase/decrease at 95% confidence. To ascertain the spatial extent of phenology change, the percentage of pixels with increasing and decreasing trends was also calculated.

$$S = \sum_{i=1}^{n-1} \sum_{j=i+1}^{n} sgn(xj - xi) \quad (5)$$

$$Z = \frac{S-1}{\sqrt{var(S)}},\ if\ S > 0;\ Z = 0,\ if\ S = 0\ and \frac{S+1}{\sqrt{var(S)}},\ if\ S < 0 \quad (6)$$

Table 1
MKZ-score classes for classifying trend test.

MKZ-score	Significance of the Trend
≥±1.96	Increase/decrease at 95% level of confidence
±1.96 to ±1.65	Increase/decrease at 95-90% level of confidence
±1.65 to ±0.83	Increase/decrease at 90-80% level of confidence
±0.83 to ±0	Increase/decrease trend but insignificant

4. Results

4.1. Spatial variations in data fusion and MODIS phenometrics

The 21-year (2000 to 2020) average crop phenology shows that data fusion (Fig. 4a-c) captured distinct spatial phenological patterns compared to MODIS (Fig. 4d-f). The subsets in Fig. 4a-f represent spatial variation in dominantly maize and Fig. 4g-i in the rice dominant fields during the study period. The spatial variability was greater for SOS than for EOS and POS. The SOS became progressively later northwards: it was earliest in the highland regions with more fragmented fields south of the study area (Dengla, south Mecha, Yilmana Densa districts) and occurred later in central Mecha and Bahir Dar Zuria, possibly as a result of the difference in the onset of rainfall and crop types. The SOS mean and standard deviation were day of year (DOY) 177±7.3 (fused) versus DOY 171.2±8.8 (MODIS). About 75% of the fused SOS pixels ranged between DOY 170 and 190, and 82% of the MODIS pixels were before DOY 180. Data fusion yielded a spatial and temporal average EOS (DOY 321±8) that was later than that obtained from MODIS (DOY 312±10.1). 92% of the fused pixels reached EOS after DOY 310, while 82% of the MODIS pixels reached EOS before DOY 320. Crops reached peak productivity (POS) at DOY 255±6.5 (fused) and at DOY 243±7.6 (MODIS). Temporally, the EVI2 signals (see supplement, Fig. S2) showed data fusion detected seasonal and inter-annual variability, and MODIS detected earlier phenology than the fused (Fig. 6) in maize and rice dominant fields over 21 years for pixels within the zoom window of Fig. 4a and d.

The maps showing the difference (in days) between the values obtained by data fusion and those obtained from MODIS (Fig. 4g-i) illustrate the spatial differences between the datasets. A larger difference between fused and MODIS occurred mainly in the fragmented and mixed crop croplands. Positive change in most of the study area shows data fusion yielded later phenology than MODIS for most of the study area (82% of SOS, 58% of POS and 88% of EOS pixels), except in the rice-growing northeast of the study area. The difference between data fusion and MODIS was about 15 days for 84% of EOS, 91% of SOS, and 98% of POS pixels. The late EOS captured by data fusion coincides with the harvest season, usually between November and mid-December. However, in the rice-dominant Fogera district, the mean SOS and EOS were earlier for MODIS than for the data fusion. This might be because flooding in the early growth stage and re-greening at EOS due to available moisture after harvest could influence the detection of phenometrics from the coarse-resolution MODIS. A greater difference and

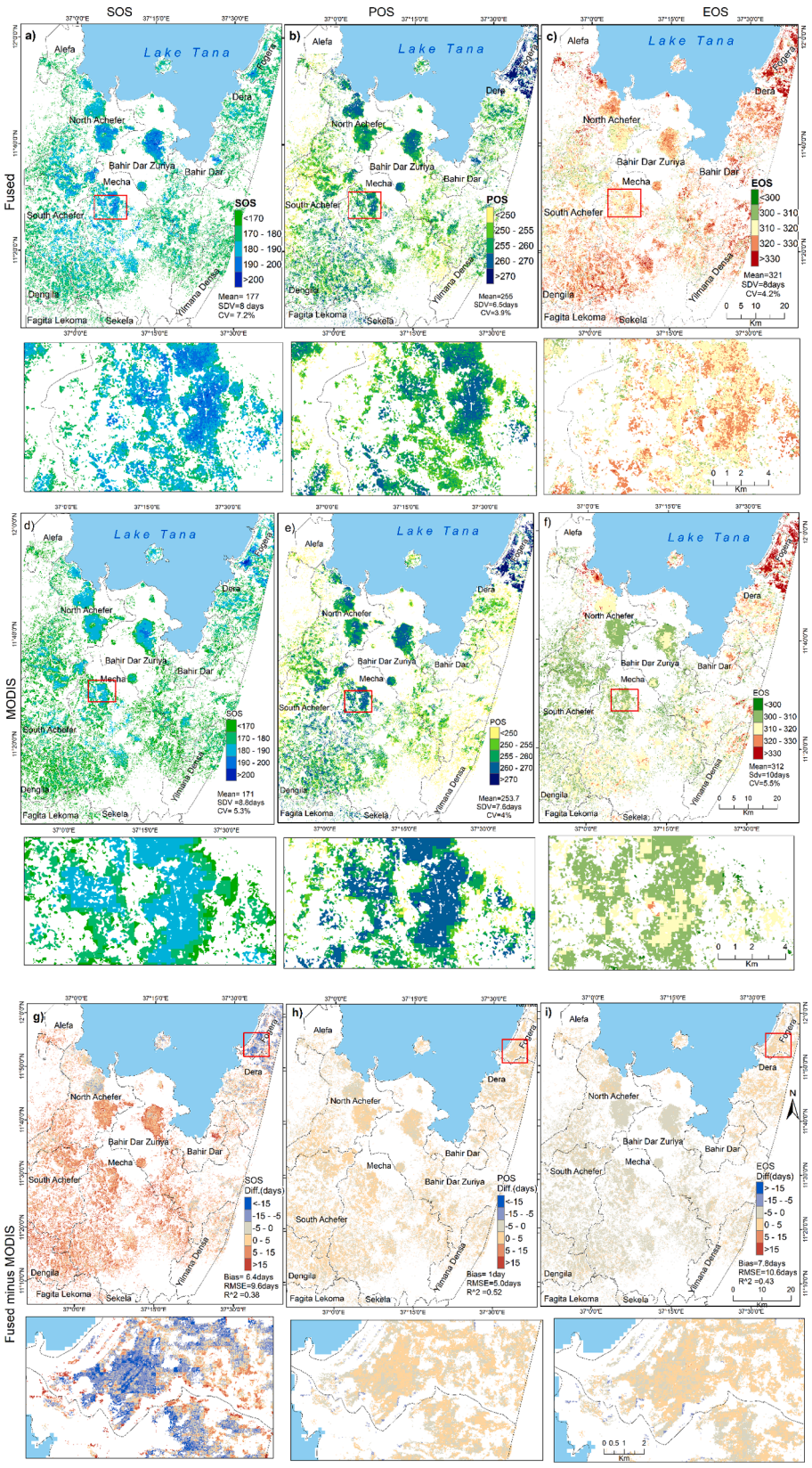

Fig. 4. Spatial distribution of the mean SOS (a), POS (b), and EOS (c) determined from fused from 2000 to 2020, and MODIS-determined SOS (d), POS (e), and EOS (f). Data fusion minus MODIS SOS (g), POS (h), and EOS (i) highlight differences. The metrics in g-i show a statistical relationship between fused and MODIS-determined phenometrics. The zoom windows focused on maize (a-f) and rice (g-i) dominant sites where the two datasets showed major differences.

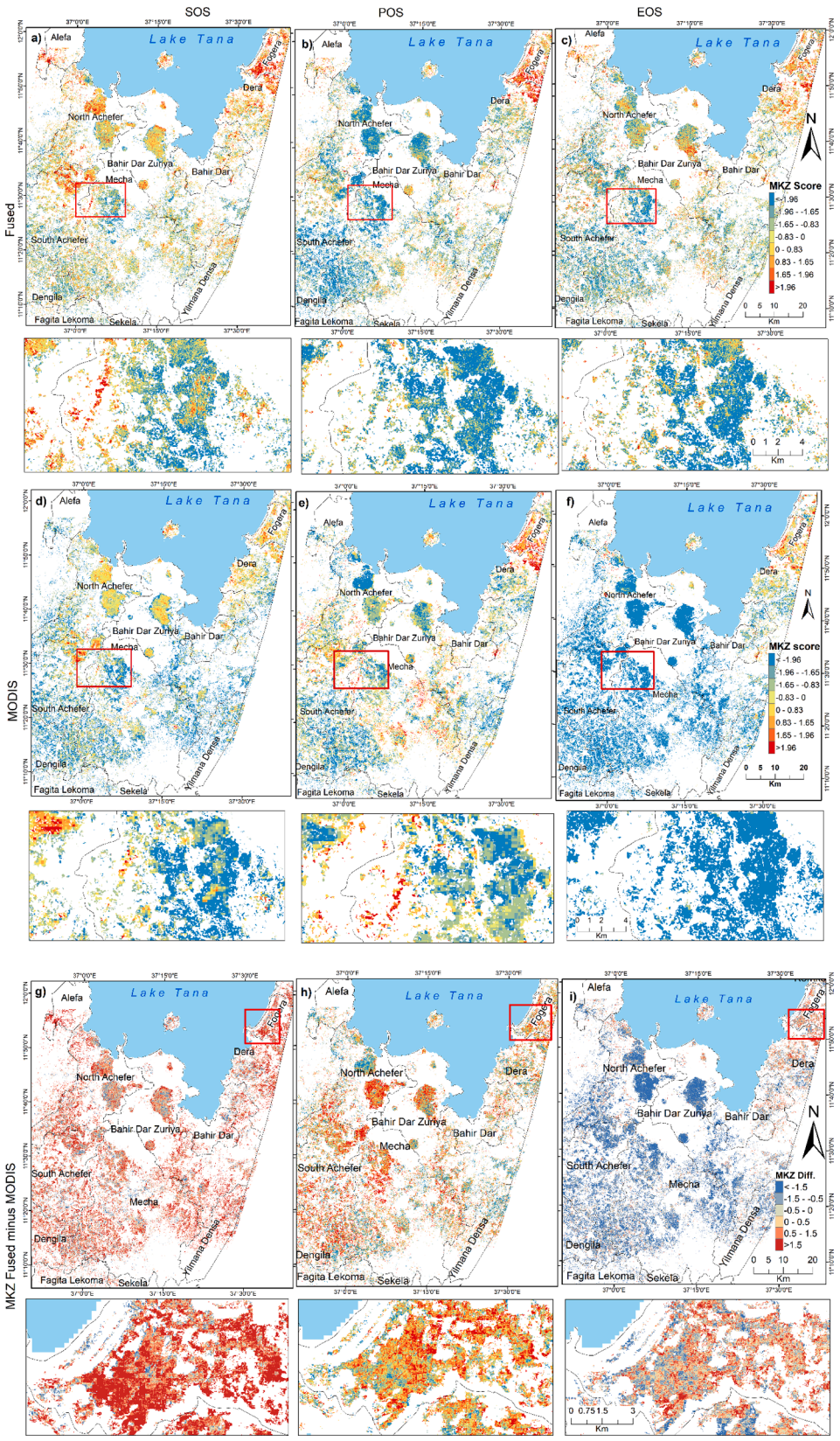

Fig. 5. Spatial distribution of significant crop phenology trends over the 21 years period. The direction of fused SOS (a), POS (b), and EOS (c) changes compared with MODIS SOS (d), POS (e), and EOS (f). The significance of change was based on the Mann–Kendall Z score (MKZ). The maps of the difference between data fusion and MODIS show the spatial distribution of fused and MODIS trend differences for SOS (g), POS (h), and EOS (i).

lower correlation between Landsat–MODIS fusion and MODIS were obtained for EOS (bias=7.8 days, RMSE=10.6 days, R^2=0.43) and the SOS (bias=6.4 days, RMSE=9.6 days, R^2=0.38), compared to POS (bias=1.0 days, RMSE=5.0 days, R^2=0.52).

4.2. Crop phenology trend retrieved from data fusion and MODIS

4.2.1. Temporal pattern of data fusion and MODIS crop phenology trend

Crop phenology trend analysis based on data fusion (Fig. 5a-c and Fig. 7a-c) and MODIS (Fig. 5d-f and Fig. 7d-f) aligned more in direction than in terms of magnitude of change in most parts of the study area. Fig. 5 shows both datasets captured crop phenology change (MKZ≠0) and a general tendency for early SOS, POS, and EOS (MKZ<0) during the study period. However, MODIS detected a higher magnitude of significant change (MKZ>1.96, p=0.05) for most parts of the study area than for the data fusion. Data fusion detected 60.2% of crop pixels that had shifted on average by -0.2±0.9 day-y^{-1} whereas MODIS captured 67.3% early SOS pixels at a magnitude of -0.5±0.6 day-y^{-1}. A statistically significantly early SOS was found for 20% of the fused pixels and 10.5% of MODIS pixels. The fused SOS retreated from DOY 190 to DOY 180 and MODIS SOS retreated from DOY 180 to DOY 170 in maize dominant sites. 76% of MODIS crop pixels showed significantly early EOS on average by -1.38±1 day-y^{-1}; the corresponding result for data fusion was 26% EOS pixels and -0.5 ±1.2 day-y^{-1}. On average, EOS shifted from DOY 325 to DOY 313 (fused) and DOY 323 to DOY 304 (MODIS). As shown in Fig. 5f, the absence of spatial variation in the magnitude of MODIS EOS trend, which is significant throughout the study area resulted in a bigger overall shift over the study period compared to the fused.

Data fusion also captured a larger proportion of significantly delayed SOS (10%) and EOS (7%) pixels than MODIS SOS (6%) and EOS (2%). Data fusion also yielded a slightly higher proportion (39.8%) and

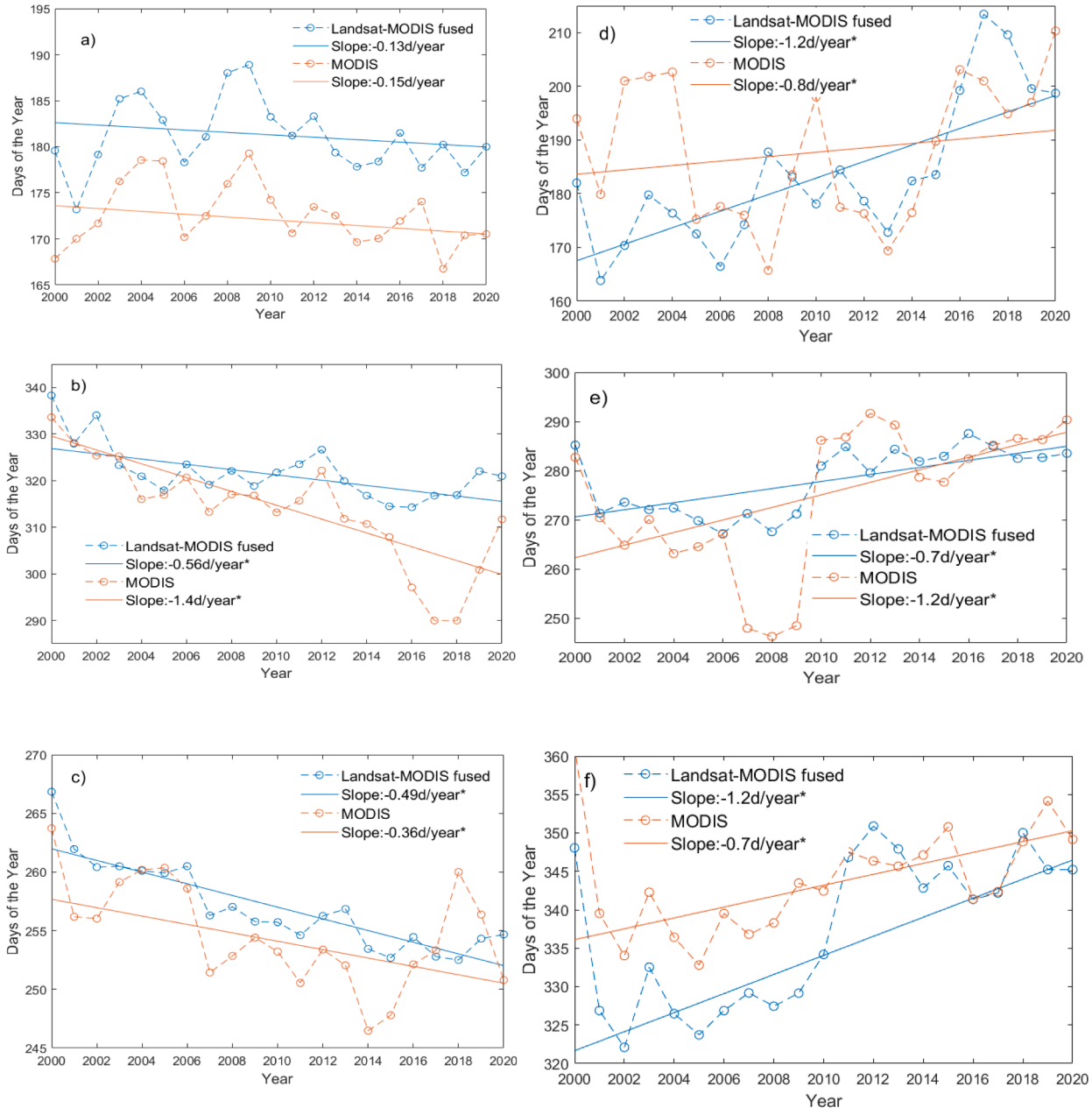

Fig. 6. Temporal pattern of phenometrics in maize (a: SOS, b: POS, and c: EOS) and rice dominant (d: SOS, e: POS, and f: EOS) pixels within the zoom area of Fig. 6a and c respectively.

magnitude (-0.51 ±0.8 day-y^{-1}) of significantly early POS than MODIS (32% and -0.36 ±0.7 day-y^{-1}). As observed in the zoom windows, data fusion captured more localized changes in the maize dominant mechanized winter irrigated farms (Fig. 5a-f) and the rice growing region (Fig. 5g-i). The mean temporal pattern of phenometrics change (Fig. 6) for crop pixels within the zoom windows showed an opposite trend in maize (earlier) and rice (delayed) growing sites in both datasets. MODIS showed large inter-annual variability in the rice region, where flooding usually influences the timing of SOS and POS detection. The result also indicates in the rice dominant site (Fig. 6d-f) data fusion detected a higher rate SOS and EOS change than MODIS.

4.2.2. *Spatial pattern of fused and MODIS crop phenology trends*

The spatial distribution in the direction of significant change (MKZ-score) in Fig. 5 and the spatial distribution of the rate of change (TS slope) in Fig. 7 showed data fusion (a-c) captured larger variations in pixel-level crop phenology trends than MODIS (d-f). For instance, MODIS detected early EOS in the entire study area (Fig. 5f), whereas data fusion revealed larger spatial variation in the direction and magnitude of significant EOS change (Fig. 5c). The datasets exhibited large differences between them and had opposing EOS trends. The spatial pattern of the fused crop phenology change was related to the spatial distribution of crop types and their growing environment. For instance, data fusion detected insignificant early SOS change (a),

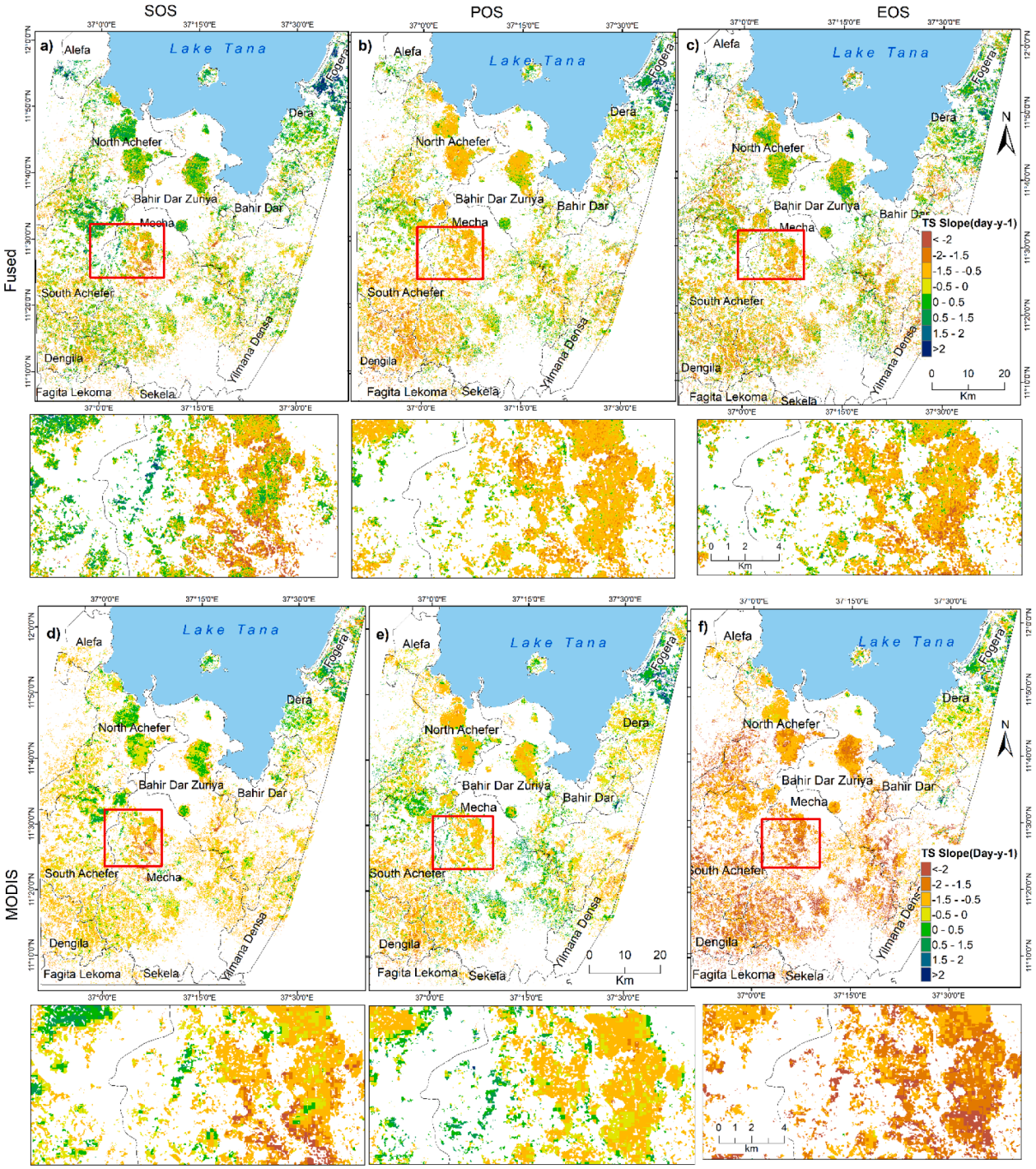

Fig. 7. The magnitude (Theil–Sen slope estimator) of crop phenology change for fused SOS (a), POS (b), and EOS (c), and MODIS SOS (d), POS (e), and EOS (f)

whereas MODIS (d) detected more significant early SOS change in most maize dominant districts south of Lake Tana. In the rice-growing region (Fogera district), fused data captured more spatial (Fig. 5a) and temporal (Fig. 6d) variation in the direction and magnitude of SOS change than MODIS (Fig. 5b and Fig. 6d), where surface water in the rice fields obscures vegetation signals in the early growth stage at MODIS spatial resolution. The trend difference map obtained by subtracting MODIS from fused (Fig. 5g-i) also showed that most of the differences between fused and MODIS were located in the highland and mixed crop growing regions (South Achefer, Dengla, Yilmana Densa districts). In these sites, the difference between the crop phenology of the coarse resolution MODIS and data fusion may have resulted from more mixed pixel issues and the early start of the rainy season. Moreover, as shown in Fig. 7, MODIS estimated a higher rate of change than fused, which resulted in a high overall rate of change.

5. Discussion

This study comprehensively investigated the longer-term crop phenology trends using Landsat and MODIS data fusion in a fragmented landscape of Ethiopia for the period 2000–2020. The four main findings were: i) Data fusion detected SOS, POS and EOS occurred later than in MODIS; ii) MODIS and data fusion showed similarities in the direction of crop phenology change, but data fusion yielded slower rates of change in SOS and EOS trend than MODIS; iii) EOS showed the highest magnitude of crop phenology change resulting in a shorter detected growing season length; and iv) data fusion captured greater per-pixel level phenology variation and environment–specific crop phenology trends than those captured by MODIS. Our findings demonstrate the feasibility and potential of longer-term (>20 years) Landsat and MODIS fusion for crop phenology trend analysis in a fragmented landscape.

5.1. Detecting time-series crop phenometrics

In general, the long-term mean crop phenometrics determined from fused data were later than those found using MODIS, because the improved spatial resolution captured crop fields. Our finding agrees with previous studies that found coarse spatial resolution Earth observation data detects earlier phenology than the high spatial resolution due to a mix of natural vegetation (Melaas et al., 2016; Qiu et al., 2020; Tian et al., 2015; Yang et al., 2020). The largest difference we found between MODIS and fused phenology was for EOS; the smallest difference was for POS. This implies the improved spatial resolution contributed to distinguishing harvested fields from senescence, which the coarse resolution MODIS lacks in fragmented agricultural landscape, consistent with the findings of Yang et al. (2020). Data fusion detected lower inter-annual variability and greater spatial variation of crop phenology than MODIS. The difference between fused and MODIS phenology occurred in the more fragmented and mixed crop-growing sites and in frequently flooded fields. Therefore, in fragmented agricultural landscapes, time-series data fusion provides an opportunity to distinguish the spatial and temporal patterns of crop phenology from the surrounding natural vegetation, which is valuable for recommending adaptation practices.

5.2. Crop phenology trend using data fusion and MODIS

In most of the study areas, MODIS and data fusion detected a similar direction of change. However, data fusion yielded smaller changes in the timing and magnitude of SOS and EOS than MODIS. For instance, MODIS EOS changed more than the fused EOS (-1.38 days/y versus -0.5days/y), and fused SOS changed more than MODIS SOS (-0.2days/y versus -0.5days/y). These high crop phenology changes deserve attention since small changes have a cascading effect on crop management practices and crop productivity for smallholder farmers (Rezaei et al., 2017). The difference between the fused and MODIS trends might be attributable to over-emphasis by the coarse resolution due to mixing with the surrounding natural vegetation of the fragmented landscape in the study area. Although we excluded non-crop pixels in the analysis, the MODIS pixels might still have contained natural vegetation that influenced the timing and magnitude of crop phenology change. In this context, Tian et al. (2013) reported that MODIS NDVI (Normalized Difference Vegetation Index) trend overestimation could be eliminated by using higher-resolution images. Through Landsat and MODIS fusion, we obtained more reasonable phenometrics timing, consistent with the crop calendar (Sisheber et al., 2022), that normalized the rate of change and captured spatial variability.

Although data fusion and MODIS agreed on the direction of SOS change, opposing trends were found in EOS, particularly in fragmented and mixed cropping locations. The fused data and MODIS also differed in capturing the rate of change in phenometrics. These differences might be related to the difference in the drivers and the likelihood of detection at Landsat and MODIS resolutions. In a rainfed system, the onset of rainfall is the main driver for SOS and for green-up in the other vegetation classes (Adole et al., 2018b), and hence the difference between MODIS and fused SOS was in the timing and magnitude rather than in the direction of change. The management after sowing greatly influences the POS and EOS. Predominantly early POS and EOS may be associated with intensive management practices such as improved varieties, fertilizers, and weed control mechanisms, all of which have been improved following government policies aimed to improve agricultural productivity since 2000 in Ethiopia (Evangelista et al., 2013; Srivastava et al., 2019). Whereas data fusion detected pixel-level variation in the direction and magnitude of EOS, MODIS did not, which could be due to the influence of natural vegetation in the MODIS pixels. In this regard, Liang et al. (2021) reported that the EOS trend in natural vegetation could be opposite to that in agricultural areas due to adaptation responses in the farmed fields. Another explanation for the early EOS in our study might be early harvesting to minimize crop loss due to earlier dry-down time after maturity thanks to improved management, similar to the finding reported by Luo and Yu (2017). Our results indicate that the spatial resolution of the data influences the timing and magnitude of the detected crop phenology change.

Unlike MODIS, the fused data detected both early and delayed EOS trends, and the variation was related to the distribution of dominant crop types and environmental differences. Our results confirm the contention that crop phenology change is environment-specific and their trend differs from natural vegetation classes (Oteros et al., 2015; Yang et al., 2020). Global and regional phenology studies in Africa focus on change in the general vegetation growth, which did not capture the changes in the fragmented croplands (Brown et al., 2012; Vrieling et al., 2013). For instance, lengthened growing seasons due to early SOS and delayed EOS have been reported in most natural vegetation classes in Ethiopia (Teferi et al., 2015; Workie and Debella, 2018). However, we found a higher magnitude of early EOS followed by POS change than the magnitude of early SOS, which has implications for a shorter growing season length. Data fusion detected large spatial and pixel-level variations in the SOS change, indicating the dataset captured management practice variations among smallholder farmers. Moreover, data fusion detects both positive and negative significant changes that imply the improved spatial resolution captured local variations that were not detected using MODIS. Therefore, the increased spatial resolution through data fusion in our study minimized the effect of the surrounding natural vegetation on crop pixels and detected a change specific to crops.

Delayed SOS, POS, and EOS were found in the rice-growing region, whereas early SOS and EOS were found in the maize and mixed crop locations, which indicates the change is crop-specific, consistent with Rezaei et al. (2017). Crop rotation and utilization of drought-resistant varieties in maize dominant sites (Srivastava et al., 2019); and resilience of rice to rainfall variability (Adhikari et al., 2015) could be attributed to crop type difference, which needs further investigation.

Moreover, the higher rainfall requirement for rice SOS than maize; increasing May and June rainfall, and frequent occurrence of flooding delayed rice phenometrics. The fused data also captured a high rate of SOS and EOS change than MODIS in rice dominant sites, where large rice field expansion occurred over the study period, implying the improved resolution contributed to detect crop type change in smallholders framing agricultural landscapes. Our previous study also confirmed that Landsat and MODIS fusion captured maize and rice phenology comparable to ground information than MODIS due to the small filed size and mixed cropping pattern in the fragmented landscape in the study area (Sisheber et al., 2022). Therefore, long-term crop phenology monitoring using data fusion could be a valuable strategy for uncovering crop type and environment-specific phenology change in fragmented crop landscapes that cannot be derived from other sources.

5.3. Contributions and limitations

To our knowledge, this study is the first to map crop phenology trends over 20+ years in a fragmented landscape using spatiotemporal Landsat and MODIS data fusion. Using the data fusion, local-scale crop phenology changes that could not be identified through coarse resolution sensors were mapped, yielding crucial information for farmers in smallholder agricultural systems. Unlike vegetation community-level investigations in previous global and regional studies, this study discerned phenological changes specific to crops from the surrounding natural vegetation in the fragmented tropical smallholder farming system, important to recommend adaptation measures. We also applied long-term data fusion to derive high spatial resolution phenology over a longer-period (21-years) that can be used to understand the effects of climate variability and climate change on crop production and estimate historical trends in crop yield that require further investigation.

One shortcoming of the study is that crop rotation and crop type could have changed during the long-term study period, thereby affecting the magnitude of the trends found. To establish that agricultural land had not changed, we used a land cover map from 2019 to mask croplands and augmented this with local knowledge of the study area. However, even when croplands remain unchanged, outliers can occur because of expansion of agricultural fields and misclassification, particularly at the boundaries of crop fields.

Although we used the smoothed phenometrics in the trend analysis, persistent cloud cover during the growing season and data fusion uncertainties could have created inter-annual variability in crop phenology detection and influenced the magnitude of crop phenology change. Taking account of historical crop type distribution could further improve data fusion to detect changes specific to crops, whilst accounting for the uncertainty introduced by cloud contaminated images in the time series.

As the time-series of high spatial resolution imagery increases, the relationship between crop phenology with climatic factors (especially rainfall and temperature) and management factors (practices, inputs and technologies) should also be explored.

6. Conclusion

This study applied longer-term (>20-years) data fusion to analyse crop phenology trend in a fragmented landscape, using the main crop-growing region of Lake Tana sub-basin, Ethiopia as a case study. Our data fusion method detected advancing crop phenology trends that require attention. The timing of the SOS, POS and EOS detected using data fusion was later than using MODIS. Although MODIS and fusion agreed on the direction of SOS, POS and EOS, data fusion detected a large significant change in the SOS and POS and spatial and temporal variability in the pattern of the EOS. Data fusion also showed a high overall rate of field level SOS, POS and EOS changes specific to crops. This improves our understanding of the changes in crop calendar in tropical smallholders farming agricultural landscapes and can guide adaptation recommendations.

Due to the mix of natural vegetation, we obtained a higher rate of SOS and EOS change using MODIS than the fused, implying higher spatial and temporal resolution is required to reveal changes specific to crops in fragmented landscapes. Furthermore, crop phenology based on data fusion contributed to detecting spatially explicit changes at field level compared to the uniform change obtained using MODIS. Our study sheds light on integrating available Earth observation data through multi-temporal Landsat and MODIS data fusion to understand crop phenology changes in fragmented agricultural landscapes.

Declaration of Competing Interest

The authors declare that they have no known competing financial interests or personal relationships that could have appeared to influence the work reported in this paper.

Data availability

Data will be made available on request.

Acknowledgments

This research was funded by the Dutch organization for internationalization in education (Nuffic), University of Twente, Faculty of Geo-information Science and Earth Observation (ITC) and Ministry of Science and Higher Education of Ethiopia (MoSHE) under the Ethiopia Education Network to Support Agricultural Transformation (EENSAT) project (Grant No: CF13198,2016). The authors would like to thank the NASA Land Processes Distributed Active Archive Center (LP DAAC) and US Geological Survey (USGS) for sharing MODIS and Landsat data. We also thank Zhu et al. for providing the ESTARFM code. Joy Burrough was the language editor of a near-final draft of the paper.

Supplementary materials

Supplementary material associated with this article can be found, in the online version, at doi:10.1016/j.agrformet.2023.109601.

References

Adhikari, U., Nejadhashemi, A.P., Woznicki, S.A., 2015. Climate change and eastern Africa: a review of impact on major crops. Food and Energy Security 4, 110–132.
Adole, T., Dash, J., Atkinson, P.M., 2018a. Characterising the land surface phenology of Africa using 500 m MODIS EVI. Applied Geography 90, 187–199.
Adole, T., Dash, J., Atkinson, P.M., 2018b. Large-scale prerain vegetation green-up across Africa. Glob Chang Biol 24, 4054–4068.
Alemu, W.G., Henebry, G.M., 2017. Land Surface Phenology and Seasonality Using Cool Earthlight in Croplands of Eastern Africa and the Linkages to Crop Production. Remote Sens 9.
Bolton, D.K., Gray, J.M., Melaas, E.K., Moon, M., Eklundh, L., Friedl, M.A., 2020. Continental-scale land surface phenology from harmonized Landsat 8 and Sentinel-2 imagery. Remote Sens Environ 240, 111685.
Brown, M.E., de Beurs, K., Vrieling, A., 2010. The response of African land surface phenology to large scale climate oscillations. Remote Sens Environ 114, 2286–2296.
Brown, M.E., de Beurs, K.M., Marshall, M., 2012. Global phenological response to climate change in crop areas using satellite remote sensing of vegetation, humidity and temperature over 26years. Remote Sens Environ 126, 174–183.
Chen, J., Liu, Y., Zhou, W., Zhang, J., Pan, T., 2021. Effects of climate change and crop management on changes in rice phenology in China from 1981 to 2010. J Sci Food Agric n/a.
Eastman, J.R., Sangermano, F., Machado, E.A., Rogan, J., Anyamba, A., 2013. Global Trends in Seasonality of Normalized Difference Vegetation Index (NDVI), 1982-2011. Remote Sens 5, 4799–4818.
Eklundh, L., Jönsson, P., 2017. TIMESAT 3.3 with seasonal trend decomposition and parallel processing Software Manual, 92. Lund University. http://www.nateko.lu.se/TIMESAT/.
Evangelista, P., Young, N., Burnett, J., 2013. How will climate change spatially affect agriculture production in Ethiopia? Case studies of important cereal crops. Clim Change 119, 855–873.

Gao, F., Anderson, M.C., Zhang, X.Y., Yang, Z.W., Alfieri, J.G., Kustas, W.P., Mueller, R., Johnson, D.M., Prueger, J.H., 2017. Toward mapping crop progress at field scales through fusion of Landsat and MODIS imagery. Remote Sens Environ 188, 9–25.
Gao, F., Hilker, T., Zhu, X.L., Anderson, M.C., Masek, J.G., Wang, P.J., Yang, Y., 2015. Fusing Landsat and MODIS Data for Vegetation Monitoring. IEEE Trans Geosci 3, 47–60.
Gummadi, S., Rao, K.P.C., Seid, J., Legesse, G., Kadiyala, M.D.M., Takele, R., Amede, T., Whitbread, A., 2018. Spatio-temporal variability and trends of precipitation and extreme rainfall events in Ethiopia in 1980-2010. ThApC 134, 1315–1328.
Hossain, M.S., Bujang, J.S., Zakaria, M.H., Hashim, M., 2015. Assessment of Landsat 7 Scan Line Corrector-off data gap-filling methods for seagrass distribution mapping. Int J Remote Sens 36, 1188–1215.
Jiang, Z.Y., Huete, A.R., Didan, K., Miura, T., 2008. Development of a two-band enhanced vegetation index without a blue band. Remote Sens Environ 112, 3833–3845.
Jong, R., Verbesselt, J., Schaepman, M.E., Bruin, S., 2012. Trend changes in global greening and browning: contribution of short-term trends to longer-term change. Global Change Biol 18, 642–655.
Knauer, K., Gessner, U., Fensholt, R., Kuenzer, C., 2016. An ESTARFM Fusion Framework for the Generation of Large-Scale Time Series in Cloud-Prone and Heterogeneous Landscapes. Remote Sens 8, 425.
Li, L., Zhao, Y.L., Fu, Y.C., Pan, Y.Z., Yu, L., Xin, Q.C., 2017. High Resolution Mapping of Cropping Cycles by Fusion of Landsat and MODIS Data. Remote Sens 9, 1232.
Liang, L., Henebry, G.M., Liu, L., Zhang, X., Hsu, L.C., 2021. Trends in land surface phenology across the conterminous United States (1982-2016) analyzed by NEON domains. Ecol Appl 31, e02323.
Liu, Y.J., Qin, Y., Ge, Q.S., Dai, J.H., Chen, Q.M., 2017. Reponses and sensitivities of maize phenology to climate change from 1981 to 2009 in Henan Province. China. Journal of Geographical Sciences 27, 1072–1084.
Luo, Z.H., Yu, S.X., 2017. Spatiotemporal Variability of Land Surface Phenology in China from 2001-2014. Remote Sens 9, 65.
Marshall, M., Okuto, E., Kang, Y., Opiyo, E., Ahmed, M., 2016. Global assessment of Vegetation Index and Phenology Lab (VIP) and Global Inventory Modeling and Mapping Studies (GIMMS) version 3 products. Biogeosciences 13, 625–639.
Melaas, E.K., Sulla-Menashe, D., Gray, J.M., Black, T.A., Morin, T.H., Richardson, A.D., Friedl, M.A., 2016. Multisite analysis of land surface phenology in North American temperate and boreal deciduous forests from Landsat. Remote Sens Environ 186, 452–464.
Meroni, M., Rembold, F., Verstraete, M.M., Gommes, R., Schucknecht, A., Beye, G., 2014. Investigating the Relationship between the Inter-Annual Variability of Satellite-Derived Vegetation Phenology and a Proxy of Biomass Production in the Sahel. Remote Sens 6, 5868–5884.
Mishra, B., Busetto, L., Boschetti, M., Laborte, A., Nelson, A., 2021. RICA: A rice crop calendar for Asia based on MODIS multi year data. Int J Appl Earth Obs Geoinf 103, 102471.
Mohammed, I., Marshall, M., de Bie, K., Estes, L., Nelson, A., 2020. A blended census and multiscale remote sensing approach to probabilistic cropland mapping in complex landscapes. ISPRS J Photogramm Remote Sens 161, 233–245.
Nakalembe, C., Becker-Reshef, I., Bonifacio, R., Hu, G., Humber, M.L., Justice, C.J., Keniston, J., Mwangi, K., Rembold, F., Shukla, S., Urbano, F., Whitcraft, A.K., Li, Y., Zappacosta, M., Jarvis, I., Sanchez, A., 2021. A review of satellite-based global agricultural monitoring systems available for Africa. Global Food Security 29, 100543.
Nietupski, T.C., Kennedy, R.E., Temesgen, H., Kerns, B.K., 2021. Spatiotemporal image fusion in Google Earth Engine for annual estimates of land surface phenology in a heterogenous landscape. Int J Appl Earth Obs Geoinf 99, 102323.
Oteros, J., Garcia-Mozo, H., Botey, R., Mestre, A., Galan, C., 2015. Variations in cereal crop phenology in Spain over the last twenty-six years (1986-2012). Clim Change 130, 545–558.
Place, F., 2009. Land Tenure and Agricultural Productivity in Africa: A Comparative Analysis of the Economics Literature and Recent Policy Strategies and Reforms. World Development 37, 1326–1336.
Qader, S.H., Atkinson, P.M., Dash, J., 2015. Spatiotemporal variation in the terrestrial vegetation phenology of Iraq and its relation with elevation. Int J Appl Earth Obs Geoinf 41, 107–117.
Qiu, T., Song, C.H., Li, J.X., 2020. Deriving Annual Double-Season Cropland Phenology Using Landsat Imagery. Remote Sens 12, 15.
Rezaei, E.E., Siebert, S., Ewert, F., 2017. Climate and management interaction cause diverse crop phenology trends. Agricultural and Forest Meteorology 233, 55–70.
Roy, D.P., Kovalskyy, V., Zhang, H.K., Vermote, E.F., Yan, L., Kumar, S.S., Egorov, A., 2016. Characterization of Landsat-7 to Landsat-8 reflective wavelength and normalized difference vegetation index continuity. Remote Sens Environ 185, 57–70.
Schmidt, M., Lucas, R., Bunting, P., Verbesselt, J., Armston, J., 2015. Multi-resolution time series imagery for forest disturbance and regrowth monitoring in Queensland. Australia. Remote Sens Environ 158, 156–168.
Schmidt, M., Udelhoven, T., Gill, T., Roder, A., 2012. Long term data fusion for a dense time series analysis with MODIS and Landsat imagery in an Australian Savanna. J Appl Remote Sens 6, 18.
Sisheber, B., Marshall, M., Ayalew, D., Nelson, A., 2022. Tracking crop phenology in a highly dynamic landscape with knowledge-based Landsat–MODIS data fusion. Int J Appl Earth Obs Geoinf 106, 102670.
Srivastava, A.K., Mboh, C.M., Faye, B., Gaiser, T., Kuhn, A., Ermias, E., Ewert, F., 2019. Options for Sustainable Intensification of Maize Production in Ethiopia. Sustainability 11.
Teferi, E., Uhlenbrook, S., Bewket, W., 2015. Inter-annual and seasonal trends of vegetation condition in the Upper Blue Nile (Abay) Basin: dual-scale time series analysis. Earth System Dynamics 6, 617–636.
Tian, F., Fensholt, R., Verbesselt, J., Grogan, K., Horion, S., Wang, Y., 2015. Evaluating temporal consistency of long-term global NDVI datasets for trend analysis. Remote Sens Environ 163, 326–340.
Tian, F., Wang, Y.J., Fensholt, R., Wang, K., Zhang, L., Huang, Y., 2013. Mapping and Evaluation of NDVI Trends from Synthetic Time Series Obtained by Blending Landsat and MODIS Data around a Coalfield on the Loess Plateau. Remote Sens 5, 4255–4279.
Vrieling, A., de Leeuw, J., Said, M.Y., 2013. Length of Growing Period over Africa: Variability and Trends from 30 Years of NDVI Time Series. Remote Sens 5, 982–1000.
Wang, Q.M., Zhang, Y.H., Onojeghuo, A.O., Zhu, X.L., Atkinson, P.M., 2017. Enhancing Spatio-Temporal Fusion of MODIS and Landsat Data by Incorporating 250 m MODIS Data. Ieee Journal of Selected Topics in Applied Earth Observations and Remote Sensing 10, 4116–4123.
Whitcraft, A.K., Becker-Reshef, I., Justice, C.O., 2015a. Agricultural growing season calendars derived from MODIS surface reflectance. International Journal of Digital Earth 8, 173–197.
Whitcraft, A.K., Becker-Reshef, I., Killough, B.D., Justice, C.O., 2015b. Meeting Earth Observation Requirements for Global Agricultural Monitoring: An Evaluation of the Revisit Capabilities of Current and Planned Moderate Resolution Optical Earth Observing Missions. Remote Sens 7, 1482–1503.
Workie, T.G., Debella, H.J., 2018. Climate change and its effects on vegetation phenology across ecoregions of Ethiopia. Global Ecology and Conservation 13, e00366.
Yang, Y.J., Ren, W., Tao, B., Ji, L., Liang, L., Ruane, A.C., Fisher, J.B., Liu, J.G., Sama, M., Li, Z., Tian, Q.J., 2020. Characterizing spatiotemporal patterns of crop phenology across North America during 2000-2016 using satellite imagery and agricultural survey data. ISPRS J Photogramm Remote Sens 170, 156–173.
Yang, Y.J., Tao, B., Liang, L., Huang, Y.W., Matocha, C., Lee, C.D., Sama, M., El Masri, B., Ren, W., 2021. Detecting Recent Crop Phenology Dynamics in Corn and Soybean Cropping Systems of Kentucky. Remote Sens 13, 22.
Zhu, X.L., Chen, J., Gao, F., Chen, X.H., Masek, J.G., 2010. An enhanced spatial and temporal adaptive reflectance fusion model for complex heterogeneous regions. Remote Sens Environ 114, 2610–2623.